

## Article

# Effect of Normalizing Treatment on Mechanical Properties of AISI 441 Stainless Steel Prepared by Investment Casting

Yukun Hu, Weimin Mao \*, Pengyu Yan and Naiyong Li 

School of Materials Science and Engineering, University of Science and Technology Beijing, Beijing 100083, China; huyukun186@163.com (Y.H.); yanpy12138@163.com (P.Y.); naiyongli25@163.com (N.L.)

\* Correspondence: mao\_wm@ustb.edu.cn; Tel.: +86-010-6233-2882

**Abstract:** In this paper, AISI 441 stainless steel was investigated as a casting steel using the investment casting process (ICP). The microstructure and mechanical properties of the as-cast and normalizing treatment samples were analyzed. The results show that the tensile strength of as-cast AISI 441 prepared by ICP is 458 MPa, and the elongation is 22.7%. Normalizing treatment can improve the mechanical performance of AISI 441 prepared by ICP, but strength and elongation have a slightly decreasing trend with increasing normalizing temperature and time. The suitable normalizing treatment condition is 850 °C for 2 h. It was found that normalizing temperature and time have little effect on grain size and carbonitride. There was an increasing trend in the mean equivalent length (MEL) of the Laves phase as normalizing temperature and time increases. The effect of normalizing treatment on strength increment was mainly related to the change of the Laves phase size.

**Keywords:** AISI 441; investment casting; microstructure; Laves phase; mechanical properties



**Citation:** Hu, Y.; Mao, W.; Yan, P.; Li, N. Effect of Normalizing Treatment on Mechanical Properties of AISI 441 Stainless Steel Prepared by Investment Casting. *Metals* **2021**, *11*, 474. <https://doi.org/10.3390/met11030474>

Academic Editors: Umberto Prisco and Kim Verbeken

Received: 29 January 2021

Accepted: 11 March 2021

Published: 13 March 2021

**Publisher's Note:** MDPI stays neutral with regard to jurisdictional claims in published maps and institutional affiliations.



**Copyright:** © 2021 by the authors. Licensee MDPI, Basel, Switzerland. This article is an open access article distributed under the terms and conditions of the Creative Commons Attribution (CC BY) license (<https://creativecommons.org/licenses/by/4.0/>).

## 1. Introduction

Grade AISI 441 is a modern titanium (Ti) and niobium (Nb) stabilized ferritic stainless steel, which is usually used as deformed steel, not casting steel in its application. It is usually produced by a rolling or forging process to refine grain and improve mechanical properties. The research of AISI 441 deformed steel is mainly focused on corrosion properties [1], high-temperature mechanical properties [2], welding properties [3], surface-coating properties [4] and deformed microstructure [5]. Because AISI 441 ferritic stainless steel has higher thermal conductivity and creep-resistance than chromium (Cr)-nickel (Ni) austenitic stainless steel, it is often rolled into thin sheets and welded into thin-walled pipe fittings of exhaust systems in the automobile manufacturing field [6–8].

In practical application, a problem found in a foundry company is that during the welding process of AISI 441 stainless steel thin-wall pipe fitting with AISI 430 investment casting parts in exhaust systems, martensite can be produced in the welding heat affected zones, which can lead to casting embrittlement and seriously threaten the safety of connector parts. In order to improve the welding problem of AISI 441 thin-walled pipe fittings with the investment casting parts in automobile exhaust systems, the investment casting process (ICP) is applied to produce AISI 441 casting. Therefore, it is necessary to study the casting performance of AISI 441 deformed steel.

Studies of AISI 441 deformed steel as casting steel lack relevant references. The basic casting performance of AISI 441 steel can only refer to the study of Kang et al. [9,10] on 18 wt % Cr ferritic stainless steel by the investment casting process. In addition, Investment castings are not normally used directly, which needs normalizing or annealing heat treatment to improve the cutting performance. Depending on the actual production process of the foundry, normalizing treatment is applied to experimental AISI 441 investment casting to improve the microstructure and mechanical performance. However, the effects of normalizing treatment on AISI 441 prepared by investment casting processes lack relevant references. Considering AISI 441 belongs to a kind of Ti-Nb microalloyed stainless steel,

the research of normalizing treatment effects on Ti and Nb microalloyed stainless steels was reviewed. It can be found that the current studies of normalizing temperature and time on Ti-Nb microalloyed stainless steels are relatively simple. Gao et al. [11] studied the effects of niobium (0–0.097 wt %) and heat treatment (normalized at 900 °C and tempered at 550 °C for 2 h) on mechanical properties of low carbon cast steels, as compared to Nb-free cast steel, the yield strength and ultimate tensile strength of the microalloyed cast steel with 0.044 wt % Nb are increased to 350 MPa and 520 MPa from 290 MPa and 485 MPa, respectively. According to work by Kostryzhev et al. [12], the 0.064 wt % Nb, 0.021 wt % Ti microalloyed steel was normalized at 600 °C for 300 s in the later stage of thermal deformation, the results showed that the relative effect of precipitation strengthening on the yield stress increased with an increase in the Nb and Ti content in steel composition. With regard to high strength low alloys (HSLA) rolling plate steels containing Nb, Kejian et al. [13] added 0.010 wt % and 0.022 wt % Ti element and studied the effects of a normalizing condition of 910 °C for half an hour, the lower yield stress values and hardness levels for all Ti-Nb steels were reduced both in as-rolled and normalized conditions. Sant'anna et al. [14] found that normalizing for 30 min at 940 °C can refine the microstructure of API 5 L X65 HSLA steel (Ti: 0.07 wt %, Nb: 0.05 wt %). In terms of normalizing treatment of hot strip steel (containing Ti and Nb stabilized elements), the normalizing treatment for 30 min at 900 °C was carried out by Itman et al. [15] on 0.06 wt % Ti and 0.02 wt % Nb microalloyed hot strip steel. Itman et al. found that the normalizing treatment reduced the number of microalloying elements, which had remained in the solution after coiling to near its equilibrium value. In terms of studies on high-temperature normalizing treatment, Yin et al. [16] studied the ultra-low carbon steel (Ti: 0.006 wt %, Nb: 0.09 wt %) normalized at 1100 °C for 1 h; the nanosized MX precipitates were found to distribute densely and homogeneously in the matrix within martensitic lath. Apparently, the above works on Ti-Nb microalloyed stainless steels can provide a reference for the normalizing treatment of AISI 441 casting steel. In addition, the studies of AISI 441 as casting steel and normalizing heat treatment will expand the application field of AISI 441 and provide a reference for the subsequent research on the casting performance of deformed materials. Based on the influence of normalizing treatment on microstructure and properties of AISI 441 casting, it can also provide guidance for the preparation and application of AISI 441 investment casting with complex shapes.

Therefore, two aspects are focused on in the research; one is the mechanical properties of AISI 441 prepared by ICP, the other is the effects of normalizing treatment on microstructure and mechanical performance.

## 2. Experimental Procedures

According to the composition standard of AISI 441 deformed steel, an XY-150-type 150 kg medium-frequency induction furnace (XinYu Mechanical and Electrical Company, Xiamen, China) was used for smelting, and the chemical compositions of AISI 441 casting steel are presented in Table 1. The Ti content is controlled in 0.1–0.2 wt % by designing the melting equipment (Self-designed equipment) and adding Ti element by argon-blowing protection to reduce titanium oxides. The equilibrium solidification curve of AISI 441 casting steel was calculated by Thermal-Calc software (Tccr-Dos, Thermo-Calc Software Company, Solna, Sweden). An SWD-3 digital thermometer device (Xinjiang Nihong Casting Instrument Company, Jiande, China) and a Metal Lab 75/80 spectrometer (Zhujin Analytical Instruments Company, Shanghai, China) were used to measure the temperature of molten steel and adjust the composition of the elements, respectively. The pouring temperature of molten steel was set at 1580–1600 °C, and the molten steels with qualified composition were poured into the experimental mold shells, which had been pre-baked at 1200 °C for 2 h, and then the mold shells were placed in a vertical direction at the same distance to air cooling. The mold shell is shown in Figure 1. As the AISI 441 steel was prepared by the investment casting process (ICP), AISI 441 ICP abbreviation is used in the following text.

**Table 1.** Chemical compositions of the AISI 441 prepared by investment casting process (ICP) (wt %).

C	N	Si	Ti	Nb	Cr	P	S	Mn	Fe
0.022	0.028	0.72	0.16	0.54	18.1	0.028	0.009	0.60	Bal.

**Figure 1.** Mold shell used in the experiment.

The as-cast samples of AISI 441 stainless steel prepared by the investment casting process were cut into round rods (15 mm in diameter and 180 mm in length). These rods were normalized in a KXS2-10-16 rapid heating furnace (Changcheng Electric Furnace Company, Changsha, China). The normalizing temperature was set at 800, 850 and 900 °C, and the normalizing time was set to 1, 2 and 3 h, respectively. The normalized round bars of the AISI 441 ICP were processed into the tensile test bars of 12 mm in diameter and 140 mm in length, and were stretched at room temperature on a WEW×300B equipment (Fangyuan Testing Machine Company, Jinan, China). The metallographic surfaces were the cut areas corresponding to the as-cast and normalized samples of the AISI 441 ICP after etched by a 50% aqua regia solution. The metallographic diagrams were photographed by MV6000 metallographic microscope (Lianchuang Analysis Instrument Manufacturing Company, Nanjing, China) and OLS4000 laser confocal microscope (Olympus, Tokyo, Japan). Quanta250 scanning electron microscope equipped with energy-dispersive spectroscopy (FEI, Hillsboro, OR, USA) was used to get scanning diagrams and characterization analysis. Image-Pro Plus software (6.0, Media Cybernetics, Rockville, MD, USA) was utilized to analyze the microstructure and precipitates in metallographic diagrams and scanning diagrams.

### 3. Results and Discussions

#### 3.1. Influences on Mechanical Properties

The trend of the tensile strength after normalizing treatment is shown in Figure 2. The corresponding changes in yield strength and elongation are given in Table 2. Based on the as-cast AISI 441 ICP mechanical properties at room temperature (tensile strength: 458 MPa, Yield strength: 260 MPa, elongation: 22.7%). The maximum and the minimum tensile strength after normalizing treatment is 522.5 MPa, 487.5 MPa, respectively, which can be increased by 14% and 6%, respectively, than that of the as-cast state, and the yield strength is also improved. Comparing with the cold-rolled 1.4509 (AISI 441) steel [17], the tensile strength of 1.4509 (AISI 441) in the rolling direction is 479–488 MPa, which is higher than that of the as-cast in this study, but the tensile strength of the AISI 441 ICP can be enhanced by normalizing treatment.

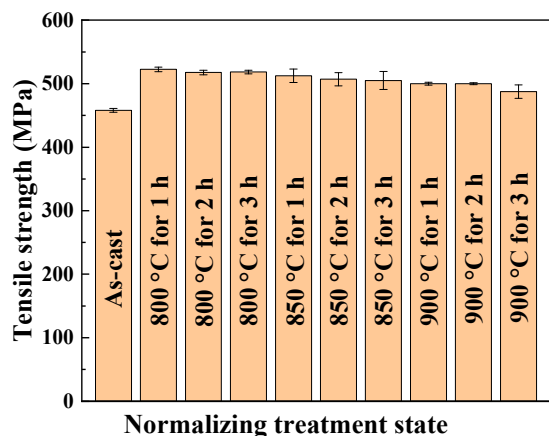


Figure 2. Variation of the tensile strength of the AISI 441 ICP after normalizing treatment.

Table 2. Mechanical properties at room temperature of the AISI 441 ICP after normalizing treatment.

State	Yield Strength (MPa)	Elongation (%)	
As-cast	260 ± 6.1	22.7 ± 5.7	
Normalizing treatment	800 °C for 1 h	290 ± 14.1	24.3 ± 3.9
	800 °C for 2 h	295 ± 2.4	21.5 ± 1.5
	800 °C for 3 h	300 ± 13.2	20.3 ± 2.8
	850 °C for 1 h	295 ± 14.1	24.3 ± 4.6
	850 °C for 2 h	315 ± 5	20 ± 11.3
	850 °C for 3 h	292.5 ± 3.5	17.8 ± 9.5
	900 °C for 1 h	302.5 ± 10.6	19 ± 6.4
	900 °C for 2 h	300 ± 7.1	20.5 ± 1.9
	900 °C for 3 h	292.5 ± 3.5	16.3 ± 2.5

It can also be seen in Figure 2 that the tensile strength of the AISI 441 ICP has a tendency to decrease with increasing normalizing temperature and time, which indicates that the increase of normalizing temperature and time cannot continue to improve the tensile strength of the AISI 441 ICP, the main reason for this change is related to the changes of microstructure. The overall trend of elongation is decreasing with a minimum value of 16.3% at 900 °C for 3 h, as shown in Table 2, but the elongation can still be maintained at 20% at 850 °C for 2 h, which is close to that of the as-cast. Figure 3 is the tensile fracture of the AISI 441 ICP. The tensile fracture surfaces of normalizing treatment at 800, 850 and 900 °C for 2 h are distributed with different sizes of dimples. As the increase of normalizing temperature, the area of dimples decreases, while the area of the fluvial pattern increases, as shown in Figure 3c; this is in accordance with the change of strength decrease. Based on the mechanical properties at room temperature, the normalizing temperature of 850 °C is the appropriate normalizing temperature. Considering the relationship between strength and plasticity, the appropriate normalizing time is 2 h.

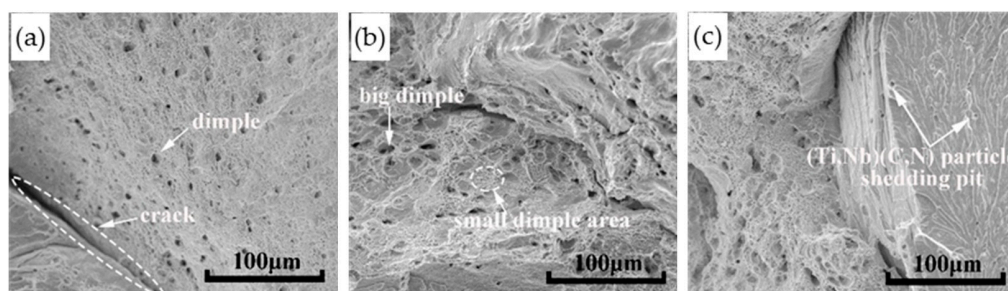


Figure 3. Tensile fracture of the AISI 441 ICP after normalizing treatment. (a) 800 °C for 2 h (b) 850 °C for 2 h (c) 900 °C for 2 h.

### 3.2. Effects of Microstructure on Mechanical Properties

#### 3.2.1. Effects by Grain Size

The grain size is shown in Table 3. It is noted that the grain size of the investment casting of AISI 441 steel has not grown abnormally after normalizing treatment. The average value of grain size under different normalizing conditions is 0.74 mm, and only a slight increase than the as-cast value of 0.70 mm. The slight increase is related to the uneven distribution of precipitates; the restriction or hindrance effects on grain migration will be reduced when the number of precipitates in grains or at the grain boundaries is relatively small, and then lead to a slight increase in the size of some grains. Since the grain size increases after normalizing treatment is slight, and the difference in grain distribution before and after normalizing treatment is not obvious, as shown in Figure 4, it can be considered that the normalizing temperature and time in this experiment have little effect on grain size.

**Table 3.** Effect of grain size on strength increment.

State	Grain Size (mm)	$\Delta YS_G$ (MPa)
As-cast	$0.70 \pm 0.07$	20.80
Normalizing treatment	800 °C for 1 h	$0.74 \pm 0.04$
	800 °C for 2 h	$0.73 \pm 0.06$
	800 °C for 3 h	$0.73 \pm 0.08$
	850 °C for 1 h	$0.75 \pm 0.05$
	850 °C for 2 h	$0.71 \pm 0.08$
	850 °C for 3 h	$0.73 \pm 0.05$
	900 °C for 1 h	$0.76 \pm 0.09$
	900 °C for 2 h	$0.74 \pm 0.08$
	900 °C for 3 h	$0.76 \pm 0.06$

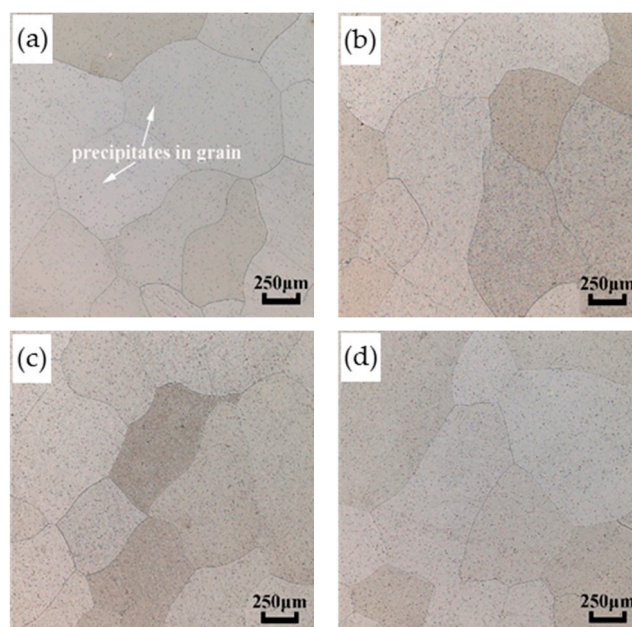


**Figure 4.** Metallographic diagrams of the AISI 441 ICP before and after normalizing treatment. (a) As-cast (b) 800 °C for 2 h (c) 850 °C for 2 h (d) 900 °C for 2 h.

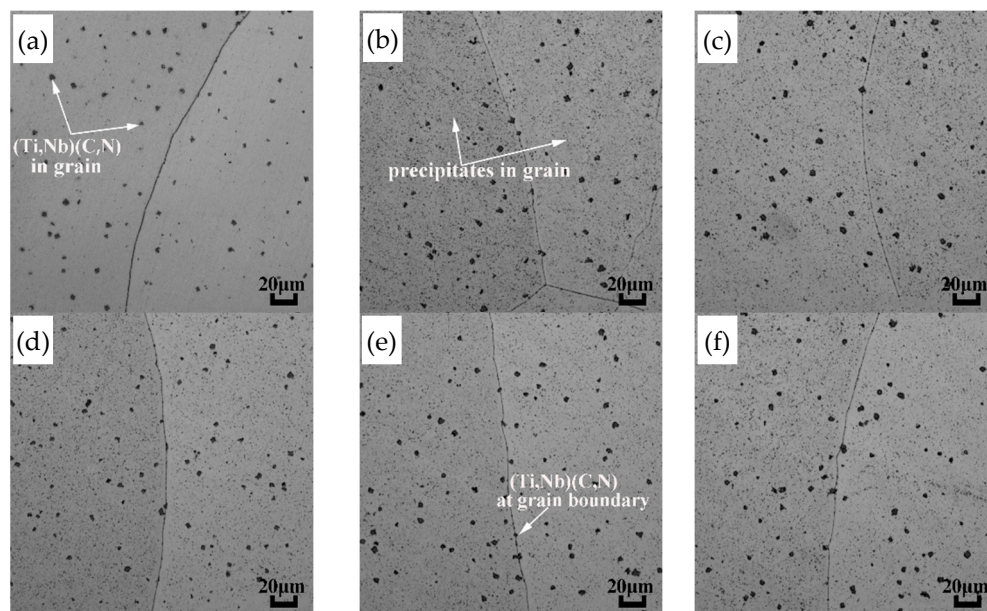
According to the relationship of Hall–Petch formula:

$$\Delta YS_G = k_y D^{-1/2} \quad (1)$$

where  $\Delta YS_G$  is the increment of yield strength,  $k_y$  is  $17.4 \text{ MPa} \cdot \text{mm}^{1/2}$  in the steel and iron material [18],  $D$  is the grain diameter. The calculation results are shown in Table 3. There is little fluctuation in the calculation values, which indicates that different normalizing temperatures and times have little effect on strength increment. The grain size after normalizing treatment is not the main factor to improve the strength.

### 3.2.2. Effects by (Ti,Nb) (C,N) Precipitates

The (Ti,Nb) (C,N) particles in the microstructure before and after normalizing treatment are shown in Figure 5, and the MEL statistics of (Ti,Nb) (C,N) particles are presented in Table 4. These (Ti,Nb) (C,N) are dispersed in grains and at the grain boundaries with the size of  $8.11 \mu\text{m}$  in the as-cast state compared with the size ranging from  $7.93 \mu\text{m}$  to  $8.16 \mu\text{m}$  of normalizing treatment state; it shows that the MEL of (Ti,Nb) (C,N) particles under different normalizing treatments is still close to that of the as-cast state. As the (Ti,Nb) (C,N) particles belong to high-temperature precipitations [19], the dissolution temperature calculated by Thermal-Calc software of Ti (C,N) and Nb (C,N) precipitates is  $1497 \text{ }^\circ\text{C}$  and  $1281 \text{ }^\circ\text{C}$ , respectively. It is also pointed out that TiN or Nb (C,N) precipitates are hardly dissolved even in the temperature range of  $900\text{--}1000 \text{ }^\circ\text{C}$  [20]. It can be seen that the normalizing temperature and time have little effect on the size of (Ti,Nb) (C,N) particles.

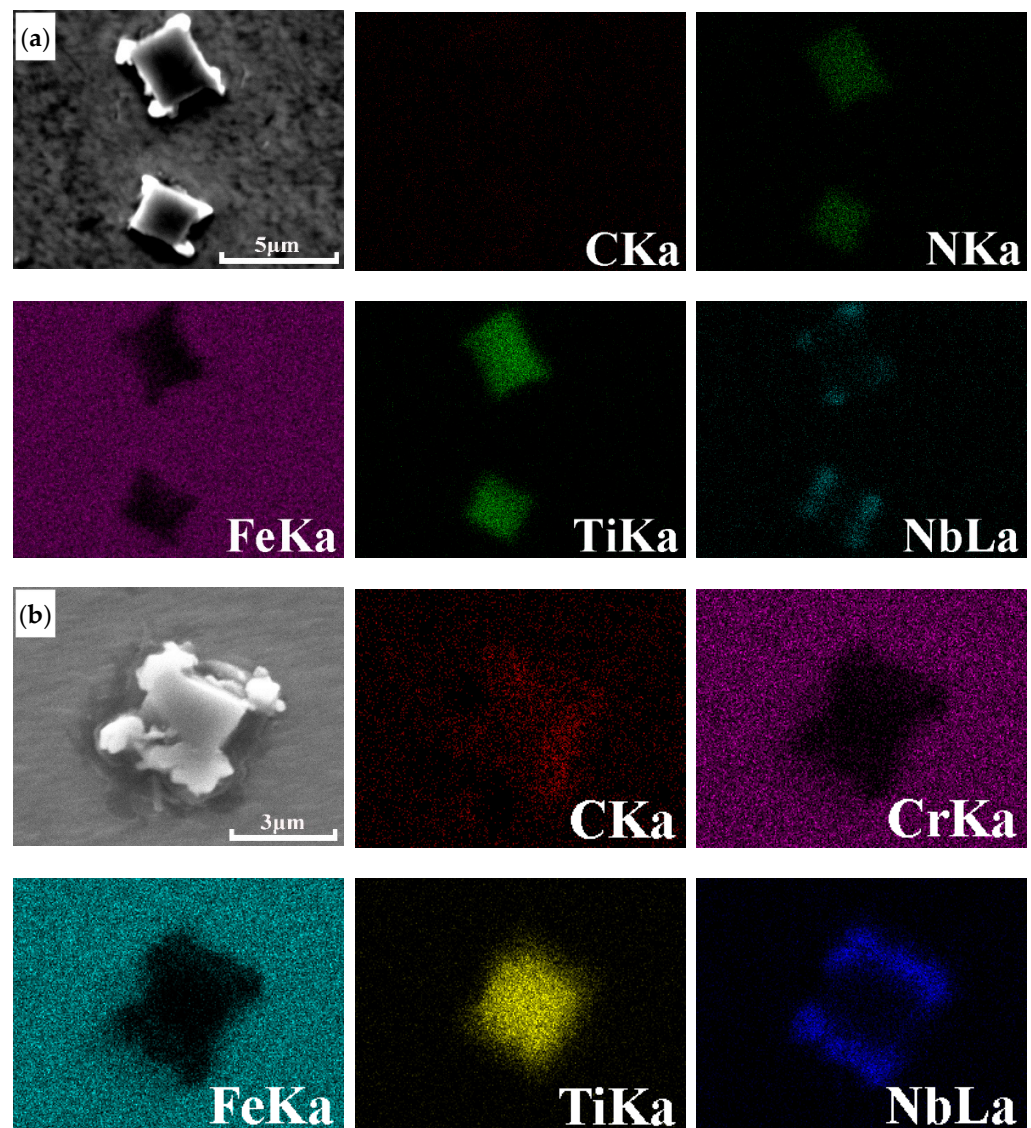


**Figure 5.** Distribution of (Ti,Nb) (C,N) particles in the AISI 441 ICP before and after normalizing treatment. (a) As-cast (b)  $800 \text{ }^\circ\text{C}$  for 2 h (c)  $850 \text{ }^\circ\text{C}$  for 2 h (d)  $900 \text{ }^\circ\text{C}$  for 1 h (e)  $900 \text{ }^\circ\text{C}$  for 2 h (f)  $900 \text{ }^\circ\text{C}$  for 3 h.

The microcosmic morphology and element distribution of (Ti,Nb) (C,N) particles are illustrated in Figure 6. The Nb (C,N) is distributed around the main body Ti (C,N) in the form of small irregular particles before and after normalizing treatment. The reason for this change is that the precipitates of Nb (C,N) and Ti (C,N) have the same face-centered cubic structures and the similar lattice parameter [21], Ti (C,N) has a lower solubility than Nb (C,N) and will form first during the cooling process from the melt, while the Nb (C,N) forms at slightly lower temperatures by heterogeneous nucleation on the existing Ti (C,N) [22]. Craven et al. [23] also observed the (Ti,Nb) (C,N) was the most common precipitate complexes found in Ti–Nb Al-killed microalloyed HSLA steels.

**Table 4.** MEL statistics of (Ti,Nb) (C,N) precipitates in the AISI 441 ICP.

State		MEL ( $\mu\text{m}$ )
As-cast		$8.11 \pm 2.58$
Normalizing treatment	800 °C for 1 h	$7.95 \pm 3.21$
	800 °C for 2 h	$8.13 \pm 2.59$
	800 °C for 3 h	$7.97 \pm 2.78$
	850 °C for 1 h	$7.93 \pm 3.19$
	850 °C for 2 h	$8.16 \pm 2.74$
	850 °C for 3 h	$8.11 \pm 3.56$
	900 °C for 1 h	$8.13 \pm 3.55$
	900 °C for 2 h	$8.13 \pm 2.45$
900 °C for 3 h	$8.14 \pm 2.87$	

**Figure 6.** Elements distribution of (Ti,Nb) (C,N) particles in the AISI 441 ICP in (a) as-cast state (backscattered electron mode) and (b) normalized state at 900 °C for 3 h (secondary electron mode).

According to Ashby–Orowan formula [24]:

$$\Delta\sigma_s = \left( \frac{0.538Gb f^{1/2}}{d} \right) \ln \left( \frac{d}{2b} \right) \quad (2)$$

where  $\Delta\sigma_s$  is the increment of yield strength (MPa),  $f$  is the volume fraction of second phase particles,  $d$  is the size of the particle (mm),  $G$  is Young's modulus, the value is 82 GPa [25,26],  $b$  is the Burgers vector, and the value is 0.248 nm [27,28]. According to Formula (2), because (Ti,Nb) (C,N) particle belongs to high-temperature precipitates, and the normalizing temperature is lower than the dissolution temperature of (Ti,Nb) (C,N) particle. There is no change in size before and after normalizing treatment, which makes the volume fraction of the (Ti,Nb) (C,N) particle unchanged. The volume fraction and the size of (Ti,Nb) (C,N) particle are quantitative values. It can be inferred that  $\Delta\sigma_s$  is not changed significantly after normalizing treatments.

### 3.2.3. Effects by the Laves Phase Precipitates

In addition to the (Ti,Nb) (C,N) precipitates in the AISI 441 ICP, there are smaller precipitates (the main component is the Laves phase [22,29,30] with a type of  $(\text{FeCrSi})_2\text{Nb}$  [31]) in grains and at the grain boundaries. The composition of the Laves phase in the experiment was verified by Energy-Dispersive Spectroscopy (EDS) analysis. The equilibrium solidification curve of the Laves phase calculated by the Thermal-Calc software is shown in Figure 7, indicates that the Laves phase belongs to the relatively low-temperature precipitation as the dissolution temperature is 987 °C. The normalizing temperature can affect the morphology and size of the Laves phase from the perspective of the equilibrium solidification curve in Figure 7.

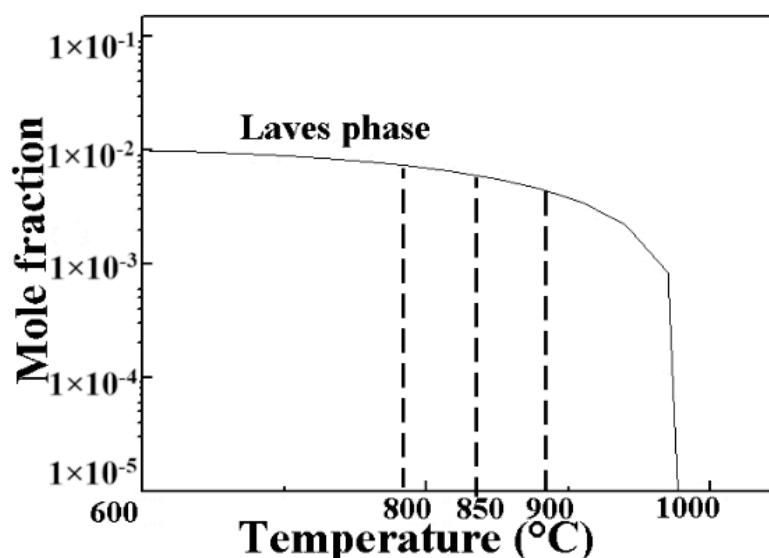
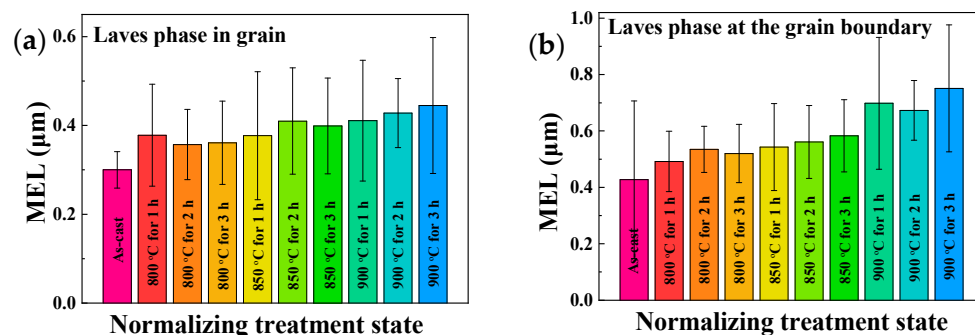


Figure 7. Equilibrium solidification curve of the Laves phase in the AISI 441 ICP.

It is shown in Figure 8 that the MEL of the Laves phase in grain and at the grain boundary is increasing with the increase of normalizing temperature and time, for example, the MEL of the Laves phase in grain is 0.36, 0.40 and 0.45  $\mu\text{m}$  at 800, 850 and 900 °C for 3 h, respectively, which is greater than that of the as-cast (0.3  $\mu\text{m}$ ). In addition, the MEL of Laves phase at the grain boundary is 0.54, 0.56 and 0.58  $\mu\text{m}$  under 850 °C with the normalizing holding time 1, 2 and 3 h respectively, which is also higher than that of the as-cast (0.43  $\mu\text{m}$ ). The other change shown in Figure 8 is that the increased range of the Laves phase size at the grain boundary is higher than that in grain, especially at 900 °C. the Laves phase at the grain boundary at 900 °C has a trend of coarsening. It can be inferred that the increase of the Laves phase is affected by normalizing conditions. The main reason is related to the

incoherent interface between Laves phase and the Fe matrix, and the coarsening rate of  $\text{Fe}_2\text{Nb}$  is much faster than that of NbC [32]. In terms of the morphology of the Laves phase after normalizing treatment, which is changed from mainly particle state to short-rod and long-rod state, as shown in Figure 9.



**Figure 8.** Mean equivalent length (MEL) of the Laves phase precipitates (a) in grain and (b) at the grain boundary of the AISI 441 ICP.

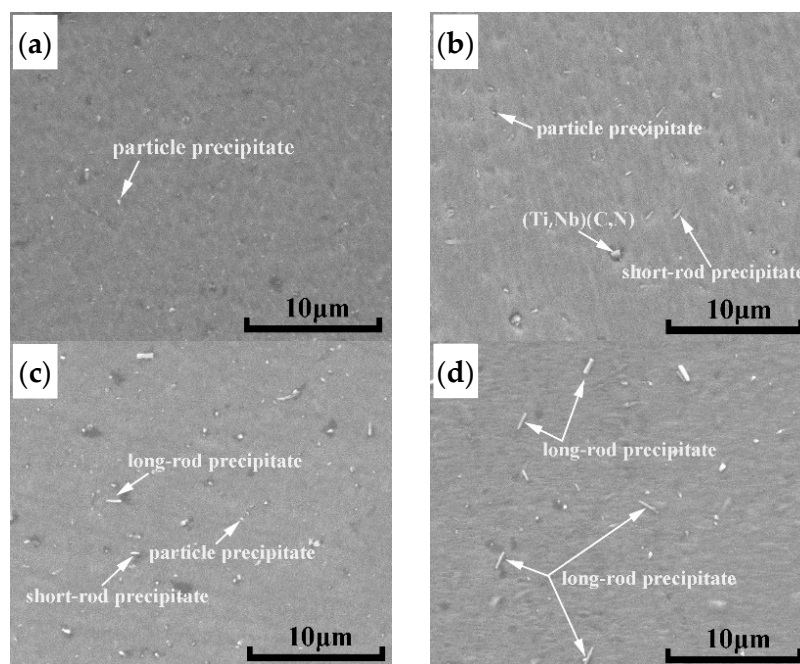


**Figure 9.** Distribution of the Laves phase precipitates in grains of the AISI 441 ICP at different normalizing temperatures. (a) as-cast (b) 800 °C for 3 h (c) 850 °C for 3 h (d) 900 °C for 3 h.

In order to calculate the value of  $\Delta YS_G$  in Equation (2), it is necessary to know the volume fraction of the Laves phase in the AISI 441 ICP sample. If the area fraction of the Laves phase in the scanning diagram is used instead of the volume fraction, the accuracy of calculation results will be reduced, and it cannot better reflect the actual influence of the Laves phase on strength increment. As the size of the Laves phase increases with increasing normalizing temperature and time, it is found that the number of the Laves phase has a decreasing trend with the increase of the Laves phase size by observing in Figure 9. On the contrary, when the size of the Laves phase is small, the number of the Laves phase is relatively increased, as shown in Figure 9c,d. The size and number of the Laves phase change similarly in Figures 10c and 11a. Since the Nb content in the AISI 441 steel is constant (0.54 wt %), the volume fraction of the Laves phase formed in the AISI 441 steel fluctuates in a stable range. The volume fraction increases correspondingly with the increasing size of the Laves phase, which makes the value of  $\Delta YS_G$  increases.

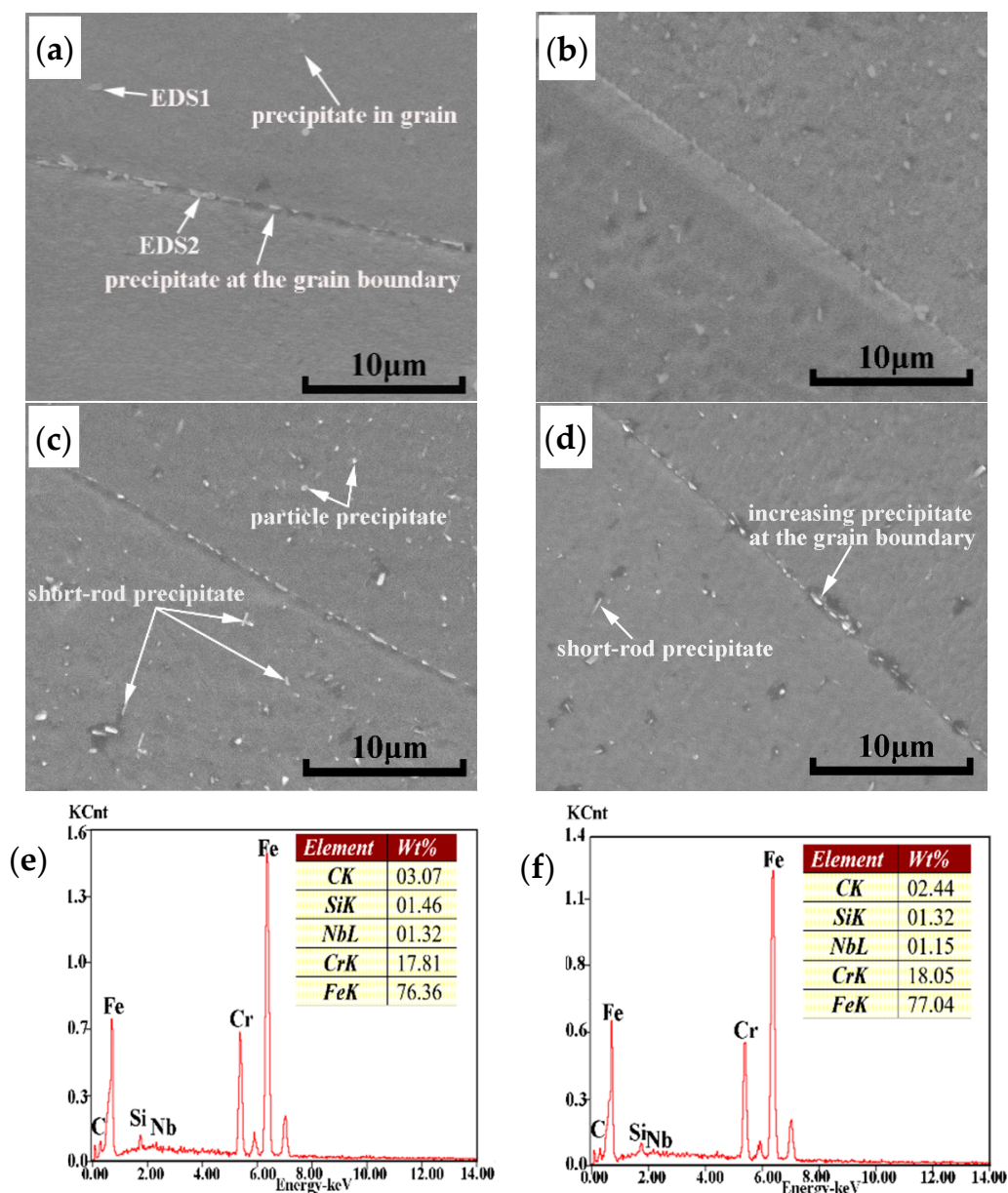


**Figure 10.** Distribution of the Laves phase precipitates and energy spectrum of the AISI 441 ICP at different normalizing times. (a) as-cast (b) 850 °C for 1 h (c) 850 °C for 2 h (d) 850 °C for 3 h (e) EDS1 energy spectrum (f) EDS2 energy spectrum.

In addition, it can be seen from the above analysis that the Laves phase at the grain boundaries tends to coarsen at 900 °C, and the effect on strength increment of the Laves phase at the grain boundary is reduced. There is related research that has verified the influences by coarsening Laves phase. Sawatani et al. [20] indicated that the toughness of the hot-rolled sheet decreases as the growth of the Laves phase in number and size at the grain boundaries. Morris et al. [33] found that rapid coarsening of the Laves precipitate particles in Fe-25% Al-2% Nb alloy at higher temperatures leads to strength loss when the temperature up to 900 °C. The study of Johnson [34] also indicates that the strengthening effect in 18% Cr ferritic steels appears related to the Laves phase precipitate, which forms at elevated temperatures. In addition, Kato et al. [35] studied the 17Cr-0.5Nb-0.5Si steel after aging at 1073 K (800 °C) exceeds 0.1 ks, the results showed that the content of the Laves phase precipitates increased, and the addition of Si promoted the precipitation of the Laves phase.

Therefore, grain size and carbonitrides have little effect on strength increment before and after normalizing treatment. The strength increment is related to the size of the Laves phase, and the contribution of the Laves phase to the strength increment is better than that of grain size and carbonitrides.

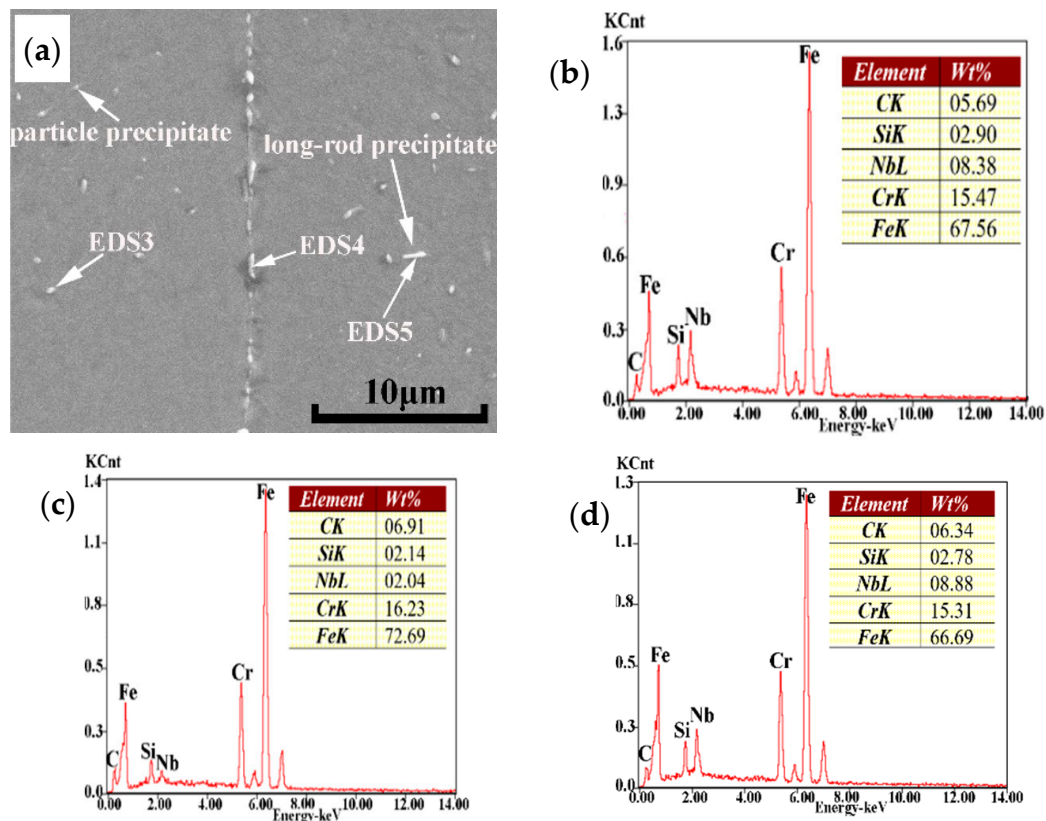


**Figure 11.** Energy spectrum of the Laves phase precipitates of the AISI 441 ICP normalized at 900 °C for 2 h. (a) Distribution of the Laves phase precipitates (b) EDS3 energy spectrum (c) EDS4 energy spectrum (d) EDS5 energy spectrum.

#### 4. Conclusions

The microstructure and mechanical properties of the as-cast and normalized AISI 441 steel using investment casting process (ICP) were investigated, the following conclusions are obtained:

1. The tensile strength of as-cast AISI 441 steel prepared by ICP is 458 MPa, and the elongation is 22.7%. Normalizing treatment can improve the mechanical performance of AISI 441 prepared by ICP;
2. Normalizing treatment condition of 850 °C for 2 h is suitable for AISI 441 steel prepared by ICP; it can effectively ensure both strength and plasticity;
3. Grain size and carbonitride are less affected by normalizing treatment, while the Laves phase tends to increase with the increase of normalizing temperature and time. The effect of the Laves phase in normalized microstructure on strength increment is higher than that of in the as-cast microstructure.

**Author Contributions:** Conceptualization, W.M.; data curation, Y.H.; methodology, P.Y.; validation, N.L. All authors have read and agreed to the published version of the manuscript.

**Funding:** This research received no external funding.

**Institutional Review Board Statement:** Not applicable.

**Informed Consent Statement:** Not applicable.

**Data Availability Statement:** The study does not report any data about publicly archived datasets analyzed or generated during the study.

**Acknowledgments:** The authors gratefully acknowledge the financial and materials support by Jiangsu Taizhou Xinyu Precision Co., Ltd. The authors would also like to express the gratitude to the Analysis and Test Center, USTB.

**Conflicts of Interest:** The authors declare no conflict of interest.

## References

1. Żuk, M.; Czupryński, A.; Czarnecki, D.; Poloczek, T. The effect of niobium and titanium in base metal and filler metal on intergranular corrosion of stainless steels. *Weld. Technol. Rev.* **2019**, *91*, 30–38. [CrossRef]
2. Prudhomme, C.; Santacreu, P.-O.; Evenepoel, I.; Proult, B. Thermomechanical fatigue behaviour of ferritic stainless steel grades for high temperatures applications. *MATEC Web Conf.* **2018**, *165*, 16003. [CrossRef]
3. Abecassis, M.; Köster, A.; Maurel, V. Short and long crack growth behavior of welded ferritic stainless steel. *Procedia Struct. Integr.* **2016**, *2*, 3515–3522. [CrossRef]
4. Limooei, M.B.; Ebrahimifar, H.; Hosseini, S. Study of the oxidation resistance of coated AISI 441 ferritic stainless steel for SOFCs. *Int. Sch. Sci. Res. Innov.* **2013**, *7*, 571–574. [CrossRef]
5. Maruma, M.G.; Siyasiya, C.W.; Stumpf, W.E. Effect of cold reduction and annealing temperature on texture evolution of AISI 441 ferritic stainless steel. *J. S. Afr. Inst. Min. Metall.* **2013**, *113*, 115–120.
6. Santacreu, P.-O.; Cleizergues, O.; Simon, C.; Duroux, P. Design of stainless steel automotive exhaust manifolds. *Rev. Métall.* **2004**, *101*, 615–620. [CrossRef]
7. Santacreu, P.-O.; Faivre, L.; Acher, A. Damage mechanisms of stainless steels under thermal fatigue. *SAE Int. J. Mater. Manuf.* **2014**, *7*, 553–559. [CrossRef]
8. Li, M.; Zhang, W.; Wang, X.; Chen, E.; Chen, C.; Zhang, H.; Shang, C. Effect of Nb on the performance of 409 stainless steel for automotive exhaust systems. *Steel Res. Int.* **2018**, *89*, 1–8. [CrossRef]
9. Kang, Y.; Mao, W.; Chen, Y.; Jing, J.; Cheng, M. Effect of Ti content on grain size and mechanical properties of UNS S44100 ferritic stainless steel. *Mater. Sci. Eng. A* **2016**, *677*, 211–221. [CrossRef]
10. Kang, Y.; Mao, W.; Chen, Y.; Jing, J.; Cheng, M. Influence of Nb content on grain size and mechanical properties of 18wt% Cr ferritic stainless steel. *Mater. Sci. Eng. A* **2016**, *677*, 453–464. [CrossRef]
11. Gao, W.; Leng, Y.; Fu, D.; Teng, J. Effects of niobium and heat treatment on microstructure and mechanical properties of low carbon cast steels. *Mater. Des.* **2016**, *105*, 114–123. [CrossRef]
12. Kostyryzhev, A.G.; Marenych, O.O.; Killmore, C.R.; Pereloma, E.V. Strengthening mechanisms in thermomechanically processed NbTi-microalloyed steel. *Met. Mater. Trans. A* **2015**, *46*, 3470–3480. [CrossRef]
13. Kejian, H.; Baker, T. The effects of small titanium additions on the mechanical properties and the microstructures of controlled rolled niobium-bearing HSLA plate steels. *Mater. Sci. Eng. A* **1993**, *169*, 53–65. [CrossRef]
14. Sant’Anna, P.C.; Rizzo, E.M.; Gomes, S.I.N.; Ferreira, I. Fracture toughness of the API 5L X65 steel submitted to intercritical heat treatments. In Proceedings of the 21st International Conference on Offshore Mechanics and Arctic Engineering, Oslo, Norway, 23–28 June 2002; Volume 7, pp. 81–86. [CrossRef]
15. Itman, A.; Cardoso, K.R.; Kestenbach, H.-J. Quantitative study of carbonitride precipitation in niobium and titanium microalloyed hot strip steel. *Mater. Sci. Technol.* **1997**, *13*, 49–55. [CrossRef]
16. Yin, F.-S.; Jung, W.-S.; Chung, S.-H. Microstructure and creep rupture characteristics of an ultra-low carbon ferritic/martensitic heat-resistant steel. *Scr. Mater.* **2007**, *57*, 469–472. [CrossRef]
17. Manninen, T.P.; Säynäjäkangas, J. Mechanical properties of ferritic stainless steels at elevated temperature. In Proceedings of the 4th International Experts Seminar on Stainless Steel in Structures, Ascot, UK, 6–7 December 2012; pp. 1–15. Available online: <https://www.researchgate.net/publication/236341600> (accessed on 3 June 2014).
18. Huo, X.D.; Mao, X.P.; Yang, Q.F.; Chai, Y.Z.; Chen, K.M. Effect of hot rolling parameters on the microstructure and properties of Ti microalloyed steel produced by compact strip production. *Iron Steel Vanadium Titan.* **2010**, *31*, 26–31. Available online: <https://doi.org/CNKI:SUN:GTFT.0.2010-02-009> (accessed on 14 April 2010). (In Chinese).
19. Fujita, N.; Ohmura, K.; Kikuchi, M.; Suzuki, T.; Funaki, S.; Hiroshige, I. Effect of Nb on high-temperature properties for ferritic stainless steel. *Scr. Mater.* **1996**, *35*, 705–710. [CrossRef]
20. Sawatani, T.; Minamino, S.; Morikawa, H. Effect of laves phase on the properties of Ti and Nb stabilized low C, N-19%Cr-2%Mo stainless steel sheets. *Trans. Iron Steel Inst. Jpn.* **1982**, *22*, 172–180. [CrossRef]
21. Fujita, N.; Ohmura, K.; Yamamoto, A. Changes of microstructures and high temperature properties during high temperature service of Niobium added ferritic stainless steels. *Mater. Sci. Eng. A* **2003**, *351*, 272–281. [CrossRef]
22. Sello, M.; Stumpf, W.E. Laves phase embrittlement of the ferritic stainless steel type AISI 441. *Mater. Sci. Eng. A* **2010**, *527*, 5194–5202. [CrossRef]
23. Craven, A. Complex heterogeneous precipitation in titanium–niobium microalloyed Al-killed HSLA steels—I. (Ti,Nb)(C,N) particles. *Acta Mater.* **2000**, *48*, 3857–3868. [CrossRef]
24. Gladman, T. Precipitation hardening in metals. *Mater. Sci. Technol.* **1999**, *15*, 30–36. [CrossRef]

25. Huang, H.; Yang, G.; Zhao, G.; Mao, X.; Gan, X.; Yin, Q.; Yi, H. Effect of Nb on the microstructure and properties of Ti-mo microalloyed high-strength ferritic steel. *Mater. Sci. Eng. A* **2018**, *736*, 148–155. [[CrossRef](#)]
26. Islamgaliev, R.; Nikitina, M.; Ganeev, A.; Sitdikov, V. Strengthening mechanisms in ultrafine-grained ferritic/martensitic steel produced by equal channel angular pressing. *Mater. Sci. Eng. A* **2019**, *744*, 163–170. [[CrossRef](#)]
27. Chen, M.Y.; Gouné, M.; Verdier, M.; Brechet, Y.; Yang, J.-R. Interphase precipitation in vanadium-alloyed steels: Strengthening contribution and morphological variability with austenite to ferrite transformation. *Acta Mater.* **2014**, *64*, 78–92. [[CrossRef](#)]
28. Rao, M.P.; Sarma, V.S.; Sankaran, S. Development of high strength and ductile ultra fine grained dual phase steel with nano sized carbide precipitates in a V–Nb microalloyed steel. *Mater. Sci. Eng. A* **2013**, *568*, 171–175. [[CrossRef](#)]
29. Sello, M.; Stumpf, W.E. Laves phase precipitation and its transformation kinetics in the ferritic stainless steel type AISI 441. *Mater. Sci. Eng. A* **2011**, *528*, 1840–1847. [[CrossRef](#)]
30. Fujita, N.; Kikuchi, M.; Ohmura, K. Expressions for Solubility Products of Fe<sub>3</sub>Nb<sub>3</sub>C carbide and Fe<sub>2</sub>Nb Laves Phase in Niobium Alloyed Ferritic Stainless Steels. *ISIJ Int.* **2003**, *43*, 1999–2006. [[CrossRef](#)]
31. Ali-Löyty, H.; Hannula, M.; Honkanen, M.; Östman, K.; Lahtonen, K.; Valden, M. Grain orientation dependent Nb–Ti microalloying mediated surface segregation on ferritic stainless steel. *Corros. Sci.* **2016**, *112*, 204–213. [[CrossRef](#)]
32. Sim, G.M.; Ahn, J.C.; Hong, S.C.; Lee, K.J. Effect of Nb precipitate coarsening on the high temperature strength in Nb containing ferritic stainless steels. *Mater. Sci. Eng. A* **2005**, *396*, 159–165. [[CrossRef](#)]
33. Morris, D.; Muñoz-Morris, M.; Baudin, C. The high-temperature strength of some Fe<sub>3</sub>Al alloys. *Acta Mater.* **2004**, *52*, 2827–2836. [[CrossRef](#)]
34. Johnson, J.N. *Influence of Columbium on the 870 °C Creep Properties of 18% Chromium Ferritic Stainless Steels*; Section 1: 810010–810234; SAE International: Warrendale, PA, USA, 1981; pp. 127–139. [[CrossRef](#)]
35. Kato, Y.; Ito, M.; Kato, Y.; Furukimi, O. Effect of Si on precipitation behavior of Nb-laves phase and amount of Nb in solid solution at elevated temperature in high purity 17%Cr-0.5%Nb steels. *Mater. Trans.* **2010**, *51*, 1531–1535. [[CrossRef](#)]